Title
Enhancement of dynamin polymerization and GTPase activity by Arc/Arg3.1

Journal
Biochimica et Biophysica Acta, 1850(6)

ISSN
0006-3002

Authors
Byers, Christopher E
Barylko, Barbara
Ross, Justin A
et al.

Publication Date
2015-06-01

DOI
10.1016/j.bbagen.2015.03.002

Peer reviewed

HHS Public Access

Author manuscript

Biochim Biophys Acta. Author manuscript; available in PMC 2016 June 01.

Published in final edited form as:

Biochim Biophys Acta. 2015 June ; 1850(6): 1310–1318. doi:10.1016/j.bbagen.2015.03.002.

Enhancement of dynamin polymerization and GTPase activity by Arc/Arg3.1

Christopher E. Byers[*], **Barbara Barylko**[*], **Justin A. Ross**[‡,1], **Daniel R. Southworth**[#,2], **Nicholas G. James**[‡], **Clinton A. Taylor IV**[*], **Lei Wang**[*], **Katie A. Collins**[§], **Armando Estrada**[*], **Maggie Waung**[§,3], **Tara C. Tassin**[*], **Kimberly M. Huber**[§], **David.M. Jameson**[‡], and **Joseph P. Albanesi**[*,4]

[*]Department of Pharmacology, University of Texas Southwestern Medical Center, Dallas, TX 75390

[§]Department of Neuroscience, University of Texas Southwestern Medical Center, Dallas, TX 75390

[‡]Department of Cell and Molecular Biology, John A. Burns School of Medicine, University of Hawaii, Honolulu, HI 9681

[#]Department of Chemistry and Chemical Biology, University of California, San Francisco, CA 94158

Abstract

BACKGROUND—The Activity-regulated cytoskeleton-associated protein, Arc, is an immediate-early gene product implicated in various forms of synaptic plasticity. Arc promotes endocytosis of AMPA type glutamate receptors and regulates cytoskeletal assembly in neuronal dendrites. Its role in endocytosis may be mediated by its reported interaction with dynamin 2 (Dyn2), a 100 kDa GTPase that polymerizes around the necks of budding vesicles and catalyzes membrane scission.

METHODS—Enzymatic and turbidity assays are used in this study to monitor effects of Arc on dynamin activity and polymerization. Arc oligomerization is measured using a combination of approaches, including size exclusion chromatography, sedimentation analysis, dynamic light scattering, fluorescence correlation spectroscopy, and electron microscopy.

RESULTS—We present evidence that bacterially-expressed His_6-Arc facilitates the polymerization of Dyn2 and stimulates its GTPase activity under physiologic conditions (37°C and 100 mM NaCl). At lower ionic strength Arc also stabilizes pre-formed Dyn2 polymers against GTP-dependent disassembly, thereby prolonging assembly-dependent GTP hydrolysis catalyzed by Dyn2. Arc also increases the GTPase activity of Dyn3, an isoform of implicated in dendrite

[4]To whom correspondence should be addressed (Joseph.Albanesi@UTSouthwestern.edu).
[1]Present address: Perkin-Elmer, Brandon Business Park, Glen Waverly, Vic, 3150, Australia
[2]Present address: Life Sciences Institute, Department of Biological Chemistry, University of Michigan, Ann Arbor, MI
[3]Present address: Department of Neurology, University of California, San Francisco, CA

remodeling, but does not affect the activity of Dyn1, a neuron-specific isoform involved in synaptic vesicle recycling. We further show in this study that Arc (either His_6-tagged or untagged) has a tendency to form large soluble oligomers, which may function as a scaffold for dynamin assembly and activation.

CONCLUSIONS and GENERAL SIGNIFICANCE—The ability of Arc to enhance dynamin polymerization and GTPase activation may provide a mechanism to explain Arc-mediated endocytosis of AMPA receptors and the accompanying effects on synaptic plasticity. This study represents the first detailed characterization of the physical properties of Arc.

Keywords

Arc/Arg3.1; dynamin; GTPase; self-assembly

INTRODUCTION

Long-term changes in synaptic strength, such as those that occur during long-term depression (LTD) and long-term potentiation (LTP) are thought to underlie learning and memory (1). A key event in both LTP and LTD is the change in the number of AMPA-type glutamate receptors (AMPARs) expressed at the postsynaptic membrane, which is accomplished through activity-dependent regulation of receptor exocytosis and endocytosis (2). Activity-dependent synaptic plasticity is also associated with rapid induction of Immediate Early Genes, including those encoding transcription factors (e.g., c-fos), growth factors (e.g., BDNF), and the protein investigated in this study, Activity-regulated cytoskeleton-associated protein (Arc (3); also known as the product of Activity-regulated gene 3.1 (Arg3.1) (4)). Arc is strongly induced by convulsive seizures, and its expression is also increased in response to neuronal activity that occurs during salient experiences, such as sensory stimulation, novelty and spatial exploration, suggesting that Arc plays a role in the synaptic changes that encode these experiences (reviewed in 5-9). In support of this idea, Arc knockout mice have deficits in LTP and LTD and in long term memory formation. Neurons from these knockout mice display increased surface expression of AMPARs, as do neurons from mice in which Arc has been depleted by RNAi treatment (10-13). Conversely, decreased surface expression of AMPARs has been observed in dissociated hippocampal neurons (11,12) or hippocampal slices (14) that over-express Arc. Therefore, it appears that one function of Arc is to stimulate internalization of the AMPAR, resulting in its relative depletion from the dendritic surface. The potential role of Arc in endocytosis is supported by the observation that Arc interacts with two elements of the endocytic machinery, endophilin and dynamin (11). Dynamins are ~100 kDa GTPases that assemble around the necks of vesiculating membranes and promote their constriction and scission (15,16). Three forms of dynamin (Dyn) are expressed in mammalian cells and all three forms are present in neurons: Dyn1 is enriched in pre-synaptic nerve terminals and promotes rapid recycling of synaptic vesicles (17); Dyn2 is ubiquitously expressed and participates in receptor-mediated endocytosis, Golgi budding, and regulation of actin polymerization (15); Dyn3 is enriched in dendritic spines and has been implicated in regulation of spine morphology (18) and stabilization of clathrin-coated pits in the vicinity of postsynaptic densities (19). The GTPase activities of dynamins are essential for endocytosis and Golgi budding (20), and Dyn2

GTPase activity was shown to be important for internalization of AMPARs (21-23). In the present study we show, using purified proteins, that Arc binding to Dyn2 accelerates its polymerization and stabilizes its assembled, high-GTPase activity state.

MATERIALS AND METHODS

Reagents

Primers were from IDT. Mouse Arc cDNA was from Thermo Scientific. pQE-80L expression vector and nickel nitrilotriacetic acid resin were from Qiagen. pGST.parallel 1 vector was a gift of Dr. Hong Zhang (UT Southwestern). His-MBP-TEV protease was a gift of Dr. Elizabeth Goldsmith (UT Southwestern). Polyclonal anti-Arc antibodies were from Synaptic Systems (Gottingen, Germany). Fluorescently labeled secondary antibodies for Infrared Imaging System were from LI-COR. Reagents for electrophoresis and immunoblotting were from Bio-Rad. [γ-^{32}P]GTP was from Perkin-Elmer. Glutathione agarose was from Pierce. Q Sepharose and other reagents, including GTP, buffers, and protease inhibitors, were from Sigma-Aldrich.

Buffers

Buffer A (lysis buffer) contained 20 mM Hepes (pH 8.0), 100 mM NaCl, 1 mM β-mercaptoethanol, 0.2 mM PMSF, and protease inhibitor cocktail. Buffer B contained 20 mM Hepes (pH 7.5), 150 mM NaCl, 0.5 mM dithiothreitol (DTT), and 0.2 mM PMSF.

Purification of His_6-tagged dynamins from S*f*9 cells

Recombinant rat dynamin 1aa (Accession number P21575), rat dynamin 2aa (Accession number P39052), and human dynamin 3a (Accession number AM393667.1) containing C-terminal His_6 tags were expressed and purified from S*f*9 cells as previously described (23-25), dialyzed against 20 mM Hepes (pH 7.5), 300 mM NaCl, 1 mM EDTA, 3 mM $MgCl_2$, 0.5 mM DTT, 0.2 mM PMSF, and stored at −70°C.

Purification of bacterially-expressed His_6-tagged Arc

Mouse Arc cDNA was introduced into the pQE-80L expression vector for bacterial production of Arc with an N-terminal RGSHHHHHHGS tag. The full-length mouse Arc clone was used as a template for preparation of His_6-tagged fragments, including Arc-N (residues 1-227), Arc-C (residues 228-396), and Arc-(Δ195-214) (deletion of residues 195-214). Full-length Arc and its fragments were purified as follows: Transformed E. *coli* were resuspended in buffer A containing lysozyme (0.05 mg/ml). The cell suspension was sonicated and centrifuged at 100,000 × *g* for 30 min at 4°C. The extract was supplemented with 30 mM imidazole and mixed with nickel nitrilotriacetic acid resin for 1 h at 4°C. The resin was washed first with buffer A containing 0.2 % Triton X-100, then with buffer A supplemented with 80 mM imidazole (pH 8.0) and 300 mM NaCl. Arc was eluted with buffer A supplemented with 150 mM imidazole (pH 8.0). After overnight dialysis of the purified protein against buffer B, aliquots were frozen in liquid N_2. The purities of proteins are shown in Supplementary Figure 1.

Preparation of untagged Arc

Mouse Arc cDNA was subcloned from the pQE-80L vector into the pGST.parallel 1 vector producing Arc with a TEV cleavage site at the N terminus. Protein was purified on glutathione resin in buffer A, washed first with 0.2% Triton X-100, then with 0.3 M NaCl (without detergent), and eluted with 50 mM glutathione. After removing glutathione by dialysis, the protein was digested with TEV at 60:1 molar ratio for 1-3 hours. Free GST and some undigested protein were removed by binding to glutathione resin. Untagged Arc (present in the supernatant) was additionally purified on Q Sepharose.

All proteins (dynamins and Arc) were centrifuged at 214,000 × *g* for 15 min at 4°C prior to all assays to remove potential aggregates.

GTPase assay

GTPase activities were measured by quantifying release of $^{32}P_i$ from [γ-^{32}P]GTP in buffer containing 20 mM Hepes (pH 7.5), 2 mM $MgCl_2$, 1 mM [γ-^{32}P]GTP and NaCl at concentrations indicated in Figure legends in a total volume of 50 µl. For short assays (0-1 min), Dyn2 was incubated alone or in the presence of His_6-Arc for 15 min at 37°C before addition of GTP to initiate the reaction. For longer assays, reaction solutions containing Dyn2 were incubated alone for 10 min at 22°C, then for another 10 min at 22°C in the presence or absence of Arc. In both cases GTPase activity was measured at 37°C and reactions were terminated by adding 750 µl of 5% (w/v) Norit in 50 mM NaH_2PO_4 (4°C) according to Higashijima et al. (27). Charcoal was removed by centrifugation and radioactivity of the 600 µl supernatant was measured by scintillation counting.

Co-sedimentation assay

Dyn2 was incubated for 15 min at 22°C in the absence or presence of His_6-Arc at 75 mM NaCl and centrifuged at 214,000 × *g* for 15 min at 22°C. The resulting pellets (P) and supernatants (S) were electrophoresed and stained with Coomassie blue. Data were quantified by intensity scanning with a ScanJet 5300C and analyzed using NIH ImageJ.

Turbidity assay

To initiate assembly, Dyn2 in buffer containing 300 mM NaCl was introduced into a 10 mm path length quartz cuvette containing either His_6-Arc in buffer B or buffer B alone and diluted with 20 mM Hepes (pH 7.5) to obtain final Dyn2, Arc, and NaCl concentrations as indicated in figure legends. Absorbances at 330 nm were measured either at 22°C (Figure 1B) or at 37°C (Figure 2) using a Beckman DU-650 spectrophotometer.

Size-exclusion chromatography

Gel filtration chromatography of untagged Arc was carried out by FPLC on HiLoad 16/600 Superdex 200 PG and His_6-Arc on HR 10/30 Superose 6 columns (GE Healthcare Life Sci.). Pre-cleared Arc solutions in buffer B were injected onto the column equilibrated and eluted with the same buffer. Elution patterns were monitored both by absorbance at 280 nm and by SDS-PAGE followed by Coomassie blue staining or by immunoblotting with anti-Arc antibody.

Density gradient centrifugation

Pre-cleared 20 μM His_6-Arc or protein standards in 0.4 ml of buffer B were layered above a 4 ml 10-40% sucrose gradient and centrifuged at 240,000 × *g* for 16 h at 4°C in a SW60 Ti rotor. Following centrifugation, sucrose concentrations were measured by refractometry.

Sedimentation velocity analysis

Sedimentation velocity measurements of His_6-Arc were performed in a Beckman XL-I analytical ultracentrifuge using the An-60 Ti rotor and 1.2-cm path length centerpieces. Data were collected at 280 nm, 20°C, and 35,000 rpm with a loading protein concentration of 36 μM in buffer B. To estimate sedimentation coefficient, five readings were averaged for each scan, and 40 scans were collected and analyzed using the second moment method in the XL-I data analysis software.

Dynamic light scattering

Dynamic light scattering measurements were performed using a Protein Solutions DynaPro instrument (Wyatt Technology). His_6-Arc samples in buffer B were centrifuged at 214,000 × *g* for 20 min immediately before measurement. Hydrodynamic radii and size distributions were calculated using Dynamics V6 software.

Fluorescence correlation spectroscopy

Single-point fluorescence correlation spectroscopy (FCS) measurements were performed using an Alba fluorescence correlation spectrometer (ISS, Champaign, IL) connected to a TE2000-U inverted microscope (Nikon, Melville, NY) with a PlanApo VC 60×1.2 NA water objective lens. Data were collected for 64 second runs with sampling rates of 256 kHz. Two-photon excitation of His_6-Arc labeled with Alexa Fluor 488 (Life Technologies, Carlsbad, CA) was provided by a Chameleon Ultra laser (Coherent, Santa Clara, CA) tuned to 800 nm. Fluorescence emission was spectrally filtered through a 680 nm short-pass filter (FF01-680; Semrock, Rochester, NY) and dichroic mirror (700dcxru; Chroma, Bellows Falls, VT). FCS of 150 nM AF488-ARC was conducted in buffer B. Data were analyzed using SimFCS (www.lfd.uci.edu). The focal spot volume was calibrated using Rhodamine 110 in water with a diffusion constant of 430 $\mu m^2/s$.

Electron microscopy

His_6-Arc in buffer B was negatively stained with uranyl formate as described (28) on 400 mesh copper grids (Pelco) coated with thin carbon film. Micrograph images were recorded using a 4k × 4k CCD camera (Gatan) at 50,000 × magnification with 2.2Å pixel size using a G2 Spirit TEM (Technai) operated at 120 keV. Single particles were selected and analyzed using *Boxer* in *EMAN* (29).

Other Methods

Protein concentration was determined using the modified Lowry method (30) according to Peterson (31) with BSA as a standard. SDS-PAGE was carried out according to Laemmli (32). Immunoblotting was performed with anti-Arc antibody detected by fluorescently labeled secondary antibody using the LI-COR Odyssey system.

RESULTS

Arc enhances Dyn2 self-assembly at physiologic ionic strength

The interaction between Arc and Dyn2 was originally identified by yeast two-hybrid analysis and was confirmed by coimmunoprecipitation of the two proteins from cell and tissue extracts (11). Using a cosedimentation assay, we verified that the purified full-length proteins are also able to interact. Binding of bacterially-expressed His_6-Arc (4 μM) to S*f*9-expressed Dyn2 polymers (1 μM) was measured, taking advantage of the ability of dynamins to self-assemble at sub-physiologic ionic strength (33). When centrifuged at 214,000 × *g* for 15 min under conditions that allow Dyn2 self-assembly (22°C, 75 mM NaCl), virtually no Arc was recovered in the pellet in the absence of Dyn2, whereas 30% of Arc pelleted in the presence of Dyn2 (Figure 1A). Quantification of the Coomassie blue-stained gels revealed that His_6-Arc not only bound to Dyn2, but also enhanced its ability to polymerize, increasing the amount of Dyn2 in the pellet from ~40% to ~80%. To determine if Arc influenced the rate as well as the extent of Dyn2 polymerization, we monitored changes in the turbidity (absorbance at 330 nm) of 0.6 μM Dyn2 solutions in the presence or absence of His_6-Arc (Figure 1B). The experiments were done at low temperature (22°C) to reduce the rate of Dyn2 polymerization and to more easily monitor the changes in turbidity after addition of Arc. In the absence of Arc, turbidity increased gradually over 600 seconds, and a pronounced lag time was evident. In the presence of 0.1 μM or 1 μM His_6-Arc the lag was no longer detectable and Dyn2 polymerization was greatly accelerated. Under these conditions, Arc by itself (at 1μM) did not self-associate into structures that increased solution turbidity.

We next asked whether Arc can induce the polymerization of Dyn2 under physiological conditions, i.e., at higher temperature and ionic strength. As shown in Figure 2C, at 37°C and 100 mM NaCl concentration, the level of turbidity in the presence of Arc was very close to that observed at lower salt and lower temperature (see Figure 1B, curve 1), but the rate of turbidity increase was dramatically higher. The turbidity of Dyn2 alone was negligible at 100 mM NaCl and 37°C.

Dynamin polymers rapidly disassemble upon addition of GTP (34). To determine if Arc affects GTP-dependent Dyn2 depolymerization, we monitored turbidity changes of Dyn2 in the absence or presence of Arc at 37°C (to accelerate dynamin polymerization) and at various salt concentrations. As expected, His_6-Arc did not detectably accelerate Dyn2 polymerization at 50 mM NaCl, a condition that by itself strongly favors Dyn2 polymerization (Figure 2A). However, Arc dramatically stabilized Dyn2 polymers against disassembly by GTP. At 75 mM NaCl, Arc not only stabilized Dyn2 polymers but also increased both the rate and extent of polymerization (Figure 2B). At 100 mM NaCl, resistance to GTP-induced disassembly of Dyn2 polymers was greatly reduced (Figure 2C). Thus, at physiologic ionic strength, Arc facilitates Dyn2 self-assembly but does not prevent GTP-dependent Dyn2 disassembly, which would be expected to suppress rather than activate endocytosis (35).

Arc stimulates the assembly-dependent GTPase activity of Dyn2 and Dyn3

The GTPase activities of dynamins are stimulated by their self-assembly into rings and coils (26, 34, 36). Therefore, it seemed likely that the enhancement of Dyn2 polymerization by His_6-Arc would be accompanied by an increase in Dyn2 GTPase activity. To test the possibility that Arc stimulates the GTPase activity of dynamin by affecting its polymerization state we performed our enzyme assays under the same conditions as those used for turbidity measurements. At 50 mM NaCl and 37°C, when Dyn2 is predominantly in the assembled state, Dyn2 alone catalyzed GTP hydrolysis at an initial rate of ~110 min^{-1}, but this rate decreased within a few seconds due to GTP-dependent disassembly of Dyn2 polymers (Figure 3A). Under the same conditions but in the presence of His_6-Arc, the initial hydrolysis rate increased slightly, to ~160 min^{-1}, and remained high during the entire one min assay, consistent with the our observation that His_6-Arc stabilizes Dyn2 polymers. The effect of His_6-Arc on Dyn2 GTPase activity was more evident when the NaCl concentration was increased to 75 mM NaCl, wherein Dyn2 by itself has much lower GTPase activity (Figures 3B). The most dramatic effect of His_6-Arc on Dyn2 GTPase activity was observed at 100 mM NaCl. In the presence of Arc, activities reached ~55 min^{-1} during the first 15 sec whereas the activity of Dyn2 alone during this interval was only ~2 min^{-1} (Figure 3C).

At 50 mM NaCl, the high-activity state of Dyn2 persisted for at least 20 min in the presence of His_6-Arc (Figure 4A). Thus, the effect of Arc on GTPase activity of dynamin mirrors its effect on dynamin assembly as measured by turbidity. Using single time point (20 min) assays, we estimated the His_6-Arc concentration dependence of GTPase activation of all three dynamin isoforms. As shown in Figure 4B, maximal activation of both Dyn2 and Dyn3 (1 μM) occurred at 0.5 μM Arc. Interestingly, His_6-Arc had no effect on the GTPase activity of Dyn1, which has a much lower propensity to self-associate than Dyn2 or Dyn3. Sedimentation and turbidity analyses confirmed that Arc induced the polymerization of Dyn2 and Dyn3 to the same extent, whereas it did not influence the assembly of Dyn1 polymers (not shown). The biphasic nature of the GTPase activation profiles is reminiscent of the activation of dynamins by PtdIns(4,5)P_2 or GST-Grb2 (37).

Arc self-associates into multiple oligomeric species

The observation that Arc promotes dynamin polymerization suggested to us that Arc itself may oligomerize, forming structures that provide a scaffold for dynamin assembly. To test this possibility we subjected purified bacterially-expressed Arc to a battery of hydrodynamic measurements. As shown in Figure 5A, untagged Arc (calculated molecular weight 45,367) displayed a broad elution pattern upon gel filtration on a Superdex 200 column, which has a nominal fractionation range for globular proteins of 10^4 to 6×10^5 Da. However, four distinct but overlapping peaks were consistently discernable. The major peak eluted near the void volume and the other three at positions corresponding to globular proteins having radii of 6.2 nm (mw ~500,000), 5.6 nm (mw ~250,000), and 4.3 nm (mw ~ 125,000). Reasonably similar results, including the presence of a 4.3 nm species, were obtained when His_6-Arc was chromatographed on a Superose 6 column, which has a fractionation range for globular proteins of 5×10^5 to 5×10^6 (Supplementary Figure 2). Thus, it is likely that the smallest Arc species eluting from gel filtration columns is either a dimer or an asymmetric monomer. Because Arc samples were cleared by high-speed centrifugation (15 min at 314 000 × *g*)

prior to chromatography, the peak eluting near the void volume does not contain large aggregates. To determine whether Arc oligomerization was reversible, we pooled and concentrated fractions containing the largest Arc species (shaded in Figure 5A) and re-chromatographed this sample on the Superdex 200 column. Figure 5B shows that the high-order oligomer clearly dissociated into lower-order species. Upon serial dilution and re-chromatography of the original Arc sample, the proportion of Arc migrating as lower-order oligomers increased (Figures 5B and 5C) further demonstrating that Arc self-association is readily reversible. Anti-Arc immunoblots of fractions eluted from Superdex 200 column runs are presented in Supplementary Figure 3.

Arc also exhibited a broad migration pattern when subjected to sucrose density gradient centrifugation (Figure 6). However, two peaks with sedimentation coefficients of ~6S and ~25 S were evident. Essentially no Arc was found in the bottom fractions of these sucrose gradients, again demonstrating the absence of exceedingly large aggregates. If we assume that the smallest species (~4.3 nm radius) from the Superdex 200 column is also the species having the lower sedimentation coefficient (6S), then we obtain a molecular weight for this species of ~108,400 (38), approximately twice the calculated molecular weight of a monomer of our Arc construct.

Although the polydispersity of our preparations prevented us from obtaining unambiguous estimates of the size and shape of Arc complexes, rigorous hydrodynamic measurements confirmed that Arc has a strong tendency to associate into high-order (yet soluble) aggregates or oligomers. For example, sedimentation velocity profiles obtained by analytical ultracentrifugation were too complex to resolve distinct oligomeric species, but indicated an average sedimentation coefficient of ~30S (Figure 7A). Dynamic light scattering (DLS) experiments yielded an average diffusion constant of 1.7×10^{-7} cm^2 s^{-1}, consistent with that of a globular protein of 13 nm radius (Figure 7B). We note, however, that for polydisperse samples such as ours, DLS is biased towards larger particles that scatter light more intensely than smaller particles. In close agreement with the DLS results, an average diffusion constant of 2×10^{-7} $cm^2 s^{-1}$ (11 nm radius) was obtained by simple fitting of fluorescence correlation spectroscopy data of Alexa-labeled Arc (Figure 7C).

Multiple Arc oligomeric species were also apparent in negatively stained electron micrographs. A portion of Arc incorporated into clusters of particles, such as those shown in the lower magnification micrograph in Figure 8A, which may correspond to the species eluting near the void volume of the gel filtration columns. Lower-order structures with radii of 2-3, 4-5, and 8-10 nm could be detected at higher magnification (Figures 8B and 8C). The 8-10 nm particles may represent the assembly units that further associate into the clusters seen in Figure 8A.

Identification of Dyn2 activation determinants in Arc

We next sought to identify regions in Arc that contribute to its ability to activate Dyn2 GTPase activity. In their initial investigation of the Arc-dynamin interaction, Chowdhury et al. (11) found that residues 195-214 in Arc were critical for dynamin binding. To determine if this segment is the sole interaction site, we generated a His_6-tagged mutant lacking these twenty residues and tested its ability to stimulate Dyn2 GTPase activity. Surprisingly,

deletion of residues 195-214 did not appreciably affect Dyn2 activation (Figure 9), indicating that Arc contains addition dynamin-binding sites. Although the three-dimensional structure of Arc has not yet been determined, sequence analysis revealed the presence of two potential domains, a coiled-coil domain (residues 49-79) and a segment (residues 228-380) bearing a weak similarity to spectrin repeat homology (SRH) domains (3). Based on this information, we generated His_6-tagged N- and C-terminal fragments consisting of residues 1-227 and 228-396, respectively (Figure 9 and Supplementary Figure 1). The N-terminal Arc fragment stimulated Dyn2 GTPase activity even more effectively than full-length Arc, whereas the C-terminal fragment failed to activate Dyn2. Thus, while residues 195-214 may contribute to dynamin binding, additional binding determinants are likely to be present in the N-terminal portion of Arc. Unfortunately, attempts to further dissect Dyn2-activation motifs in the N-terminus were unsuccessful due to the insolubility of fragments within residues 1-227.

DISCUSSION

This study provides biochemical and enzymatic evidence supporting the observation of Chowdhury et al. (11) that Arc interacts directly with Dyn2. At low ionic strength, Arc inhibited the disassembly of Dyn2 polymers by GTP, allowing GTP hydrolysis to proceed at near maximal rates for at least 20 min. At physiologic ionic strength, Arc promoted Dyn2 assembly, and accelerated GTP hydrolysis, without interfering with GTP-dependent disassembly.

Lyford et al. (3) reported that bacterially-expressed Arc was almost entirely soluble, even under relatively mild buffer conditions. This result is consistent with our observation that more than 90% of bacterially-expressed Arc (either His_6-tagged or untagged) was recovered in supernatants following high-speed centrifugation. However, our hydrodynamic data indicated that Arc self-associates into discrete low-order species (perhaps dimers), which then assemble into larger, more heterogeneous polymers. To ensure that oligomerization of Arc was not due to its association with bacterial lipids, we washed the resins with 0.2% Triton X-100 prior to Arc elution. Extensive association of Arc with bacterial nucleic acids was also unlikely, given the low ratio of absorbance at 260 vs. 280 nm of our samples (not shown). The data presented here did not allow us to assign precise subunit stoichiometries to the low-order Arc oligomers. However, the presence of these oligomers raises the possibility that Arc assembles into a multivalent scaffold that promotes dynamin polymerization.

In contrast to other *in vitro* activators of dynamin GTPase activity, such as microtubules (39) or anionic phospholipid vesicles (40), Arc stimulated the activities of Dyn2 and Dyn3 but not that of Dyn1. This finding may simply reflect the fact that Dyn1 has a much lower intrinsic propensity to self-assemble than the other two forms of dynamin (26,36), suggesting that Arc is a less potent scaffold for dynamins than microtubules or liposomes, which have a much higher valency. However, the fact that Dyn1 is predominantly expressed in presynaptic terminals, whereas Arc is absent from presynaptic terminals and axons but, like Dyns 2 and 3, is abundantly expressed in dendrites (9), may point to a more specific reason for this selectivity.

The precise role(s) of the Arc-dynamin interaction in synaptic plasticity is not yet entirely clear. An obvious possibility raised by our study is that Arc functions as a scaffold to induce the assembly of dynamin rings around the necks of budding endocytic vesicles on the dendritic plasma membrane, leading to membrane constriction and scission. However, receptor-mediated endocytosis is a process that is common to all cells, whereas Arc is selectively expressed in neurons. In addition, it is difficult to reconcile the general role of dynamins in endocytosis with the more specific effects of Arc deletion or overexpression on AMPAR internalization. An attractive scenario is one in which Arc functions as a dynamin scaffold primarily in regions of the dendritic plasma membrane, adjacent to the post-synaptic density (PSD), that are specialized for AMPAR uptake, the so-called post-synaptic "endocytic zones" (EZs; 41). Interestingly, there is evidence that EZs are physically linked to PSDs by complexes of Dyn3 and the scaffolding protein, Homer (18,19).

It should also be noted that both Arc and dynamins associate with the actin cytoskeleton. Indeed, Arc was first identified as an actin cytoskeleton binding protein (3). Thus, Arc-Dyn2 complexes may serve to stimulate actin polymerization in the vicinity of budding vesicles, which has also been implicated in the early stages of endocytosis (42). Activity-dependent remodeling of dendritic spines is largely determined by reorganization of the actin cytoskeleton (reviewed, for example, in 43). Surprisingly, Arc has been linked both to actin-dependent spine enlargement during LTP (44,45) and to an increased density and proportion of thin spines, consistent with a role in LTD (46). Perhaps these opposing activities can be explained in part by the engagement of Arc in distinct, context-dependent interactions with other proteins, including dynamins.

Supplementary Material

Refer to Web version on PubMed Central for supplementary material.

Acknowledgments

FUNDING This work was supported by National Institutes of Health grants GM076665 (DMJ) and NS045711 (KMH).

ABBREVIATIONS

AF488	Alexa Fluor 488
AMPA	α-amino-3-hydroxyl-5-methyl-4-isoxazole-propionic acid
Arc	activity regulated cytoskeleton-associated protein
DLS	dynamic light scattering
LTD	long-term depression
LTP	long-term potentiation
PtdIns(4,5)P_2	phosphatidylinositol (4,5) bisphosphate

REFERENCES

1. Bredt DS, Nicoll RA. AMPA receptor trafficking at excitatory synapses. Neuron. 2003; 40:361–379. [PubMed: 14556714]
2. Anggono V, Huganir RL. Regulation of AMPA receptor trafficking and synaptic plasticity. Curr.Opin.Neurobiol. 2012; 22:461–469. [PubMed: 22217700]
3. Lyford GL, Yamagata K, Kaufman WE, Barnes CA, Sanders LK, Copeland NG, Gilbert DJ, Jenkins NA, Lanahan AA, Worley PF. Arc, a growth factor and activity-regulated gene, encodes a novel cytoskeleton-associated protein that is enriched in neuronal dendrites. Neuron. 1995; 14:433–445. [PubMed: 7857651]
4. Link W, Konietzko U, Kauselmann G, Krug M, Schwanke B, Frey U, Kuhl D. Somatodendritic expression of an immediate early gene is regulated by synaptic activity. Proc. Natl. Acad. Sci. USA. 1995; 92:5734–5738. [PubMed: 7777577]
5. Tzingounis AV, Nicoll RA. Arc/Arg3.1: linking gene expression to synaptic plasticity and memory. Neuron. 2006; 53:403–407. [PubMed: 17088207]
6. Bramham CR, Worley PF, Moore MJ, Guzowki JF. The immediate early gene Arc/Arg3.1: regulation, mechanisms, and function. J. Neurosci. 2008; 28:11760–11767. [PubMed: 19005037]
7. Bramham CR, Alme MN, Bittins M, Kuipers SD, Nair RR, Pai B, Panja D, Schubert M, Soule J, Tiron A, Wibrand K. The Arc of synaptic memory. Exp. Brain Res. 2010; 200:125–140. [PubMed: 19690847]
8. Plath N, Ohana O, Dammermann B, Errington ML, Schmitz D, Gross C, Mao X, Engelsberg A, Mahlke C, Welzl H, Kobalz U, Stawrakakis A, Fernandez E, Waltereit R, Bick-Sander A, Therstappen E, Cooke SF, Blanquet V, Wurst W, Salmen B, Bosl MR, Lipp HP, Grant SGN, Bilss TVP, Wolfer DP, Kuhl D. Arc/Arg3.1 is essential for the consolidation of synaptic plasticity and memories. Neuron. 2006; 52:437–444. [PubMed: 17088210]
9. Shepherd JD, Bear MF. New views of Arc, a master regulator of synaptic plasticity. Nature Neurosci. 2011; 14:279–284. [PubMed: 21278731]
10. Shephard JD, Rumbaugh G, Wu J, Chowdhury S, Plath N, Kuhl D, Huganir RL, Worley PF. Arc/Arg3.1 mediates homeostatic synaptic scaling of AMPA receptors. Neuron. 2006; 52:475–484. [PubMed: 17088213]
11. Chowdhury S, Shepherd JD, Okuno H, Lyford G, Petralia RS, Plath N, Kuhl D, Huganir RL, Worley PF. Arc/Arg3.1 interacts with the endocytic machinery to regulate AMPA receptor trafficking. Neuron. 2006; 52:445–459. [PubMed: 17088211]
12. Waung MW, Pfeiffer BE, Nosyreva ED, Ronesi JA, Huber KM. Rapid translation of Arc/Arg3.1 selectively mediates mGluR-dependent LTD through persistent increases in AMPAR endocytosis rate. Neuron. 2008; 59:84–97. [PubMed: 18614031]
13. Liu Y, Zhou QX, Hou YY, Lu B, Yu C, Chen J, Ling QL, Cao J, Chi ZQ, Xu L, Liu JG. Actin polymerization-dependent increase in synaptic Arc/Arg3.1 expression in the amygdala is crucial for the expression of aversive memory associated with drug withdrawal. J. Neurosci. 2012; 32:12005–12017. [PubMed: 22933785]
14. Rial Verde EM, Lee-Osbourne J, Worley PF, Malinow R, Cline HT. Increased expression of the immediate-early gene arc/arg3.1 reduces AMPA receptor-mediated synaptic transmission. Neuron. 2006; 52:461–474. [PubMed: 17088212]
15. Praefcke GJ, McMahon HT. Thedynamin superfamily: universal membrane tubulation and fission molecules. Nat. Rev. Mol. Cell Biol. 2004; 5:133–147. [PubMed: 15040446]
16. Ramachandran R. Vesicle scission: dynamin. Semin. Cell Dev. Biol. 2011; 22:10–17. [PubMed: 20837154]
17. Ferguson SM, Brasnjo G, Hayashi M, Wolfel M, Collesi C, Giovedi S, Raimondi A, Gong LW, Ariel P, Paradise S, O'toole E, Flavell R, Cremona O, Miesenbock G, Ryan TA, De Camilli P. A selective activity-dependent requirement for dynamin 1 in synaptic vesicle endocytosis. Science. 2007; 316:570–574. [PubMed: 17463283]
18. Gray NW, Kruchten AE, Chen J, McNiven MA. A dynamin-3 spliced variant modulates the actin/cortactin-dependent morphogenesis of dendritic spines. J. Cell Sci. 2005; 118:1279–1290. [PubMed: 15741233]

19. Lu J, Helton TD, Blanpied TA, Racz B, Newpher TM, Weinberg RJ, Ehlers MD. Postsynaptic positioning of endocytic zones and AMPA receptor cycling by physical coupling of dynamin-3 to Homer. Neuron. 2007; 55:874–889. [PubMed: 17880892]
20. McNiven MA, Cao H, Pitts KR, Yoon Y. The dynamin family of mechano-enzymes:pinching in new places. Trends Biochem.Sci. 2000; 25:115–120. [PubMed: 10694881]
21. Carroll RC, Beattie EC, Xia H, Luscher C, Altschuler Y, Nicoll RA, Malenka RC, von Zastrow M. Dynamin-dependent endocytosis of ionotropic glutamate receptors. Proc. Natl. Acad. Sci. U.S.A. 1999; 96:14112–14117. [PubMed: 10570207]
22. Lin JW, Ju W, Foster K, Lee SH, Ahmadian G, Wyszynski M, Yang YT, Sheng M. Distinct molecular mechanisms and divergent endocytotic pathways of AMPA receptor internalization. Nat. Neurosci. 2000; 3:1282–1290. [PubMed: 11100149]
23. Jaskolski F, Mayo-Martin B, Jane D, Henley JM. Dynamin-dependent membrane drift recruits AMPA receptors to dendritic spines. J. Biol. Chem. 2009; 284:12491–12503. [PubMed: 19269965]
24. Lin HC, Barylko B, Achiriloaie M, Albanesi JP. Phosphatidylinositol (4,5)-bisphosphate-dependent activation of dynamins I and II lacking the proline/arginine-rich domains. J. Biol. Chem. 1997; 272:25999–26004. [PubMed: 9325335]
25. Achiriloaie M, Barylko B, Albanesi JP. Essential role of the dynamin pleckstrin homology domain in receptor-mediated endocytosis. Mol. Cell Biol. 1999; 19:1410–1415. [PubMed: 9891074]
26. Barylko B, Wang L, Binns DD, Ross JA, Tassin TC, Collins KA, Jameson DM, Albanesi JP. The proline/arginine-rich domain is a major determinant of dynamin self-activation. Biochemistry. 2010; 49:10592–10594. [PubMed: 21082776]
27. Higashijima T, Ferguson KM, Smigel MD, Gilman AG. The effect of GTP and Mg2+ on the GTPase activity and the fluorescent properties of Go. J. Biol. Chem. 1987; 262:757–761. [PubMed: 3027067]
28. Ohi MD, Li Y, Cheng Y, Walz T. Negative Staining and Image Classification - Powerful Tools in Modern Electron Microscopy. Biol. Proc. Online. 2004; 6:23–34.
29. Ludtke SJ, Baldwin PR, Chiu W. EMAN: semiautomated software for high-resolution single-particle reconstructions. J. Struct. Biol. 1999; 128:82–97. [PubMed: 10600563]
30. Lowry OH, Rosebrough NJ, Farr AL, Randall RJ. Protein measurement with the Folin phenol reagent. J. Biol. Chem. 1951; 193:265–275. [PubMed: 14907713]
31. Peterson GL. A simplification of the protein assay method of Lowry et al. which is more generally applicable. Anal.Biochem. 1977; 83:346–356. [PubMed: 603028]
32. Laemmli UK. Cleavage of structural proteins during the assembly of the head of bacteriophage T4. Nature. 1970; 227:680–685. [PubMed: 5432063]
33. Hinshaw JE, Schmid SL. Dynamin self-assembles into rings suggesting a mechanism for coated vesicle budding. Nature. 1995; 374:190–192. [PubMed: 7877694]
34. Warnock DE, Hinshaw JE, Schmid SL. Dynamin self-assembly stimulates its GTPase activity. J. Biol. Chem. 1996; 271:22310–22314. [PubMed: 8798389]
35. Pawlowski N. Dynamin self-assembly and the vesicle scission mechanism: how dynamin oligomers cleave the membrane neck of clathrin-coated pits during endocytosis. Bioessays. 2010; 32:1033–1039. [PubMed: 20957720]
36. Warnock DE, Baba T, Schmid SL. Ubiquitously expressed dynamin-II has a higher intrinsic GTPase activity and a greater propensity for self-assembly than neuronal dynamin-I. Mol. Biol. Cell. 1997; 8:2553–2562. [PubMed: 9398675]
37. Barylko B, Binns D, Lin KM, Atkinson MA, Jameson DM, Yin HL, Albanesi JP. Synergistic activation of dynamin GTPase by Grb2 and phosphoinositides. J. Biol. Chem. 1998; 273:3791–3797. [PubMed: 9452513]
38. Erickson HP. Size and shape of protein molecules at the nanometer level determined by sedimentation, gel filtration, and electron microscopy. BiolProced Online. 2009; 11:32–51.
39. Shpetner HS, Vallee RB. Dynamin is a GTPase stimuated to high levels of activity by microtubules. Nature. 1992; 355:733–735. [PubMed: 1311055]
40. Tuma PL, Stachniak MC, Collins CA. Activation of dynamin GTPase by acidic phospholipids and endogenous rat brain vesicles. J. Biol. Chem. 1993; 268:17240–17246. [PubMed: 8349610]

41. Blanpied TA, Scott DB, Ehlers MD. Dynamics and regulation of clathrin coats at specialized endocytic zones of dendrites and spines. Neuron. 2002; 36:435–449. 2002. [PubMed: 12408846]
42. Conibear E. Converging views of endocytosis in yeast and mammals. Curr.Opin. Cell Biol. 2010; 22:513–518. [PubMed: 20538447]
43. Bosch M, Hayashi Y. Structural plasticity of dendritic spines. Curr.Opin. Neurobiol. 2012; 2:383–388. [PubMed: 21963169]
44. Messaoudi E, Kanhema T, Soule J, Tiron A, Dagyte G, da Silva B, Braham CR. Sustained Arc/Arg3.1 synthesis controls long-term potentiation consolidation through regulation of local actin polymerization in the dentate gyrus in vivo. J. Neurosci. 2007; 27:10445–10455. [PubMed: 17898216]
45. Bramham CR. Local protein synthesis, actin dynamics, and LTP consolidation. Curr.Opin.Neurobiol. 2008; 18:524–531. [PubMed: 18834940]
46. Peebles CL, Yoo J, Thwin M, Palop JJ, Noebels JL, Finkbeiner S. Arc regulates spine morphology and maintains network stability in vivo. Proc. Natl. Acad. Sci. U.S.A. 2010; 107:1813–18178. [PubMed: 20133829]

Highlights for Review

- Arc binds to dynamin 2 and promotes its polymerization.
- Arc stabilizes dynamin polymers against GTP-dependent disassembly.
- GTPase activation is prolonged in Arc-stabilized dynamin polymers.
- The N-terminal portion of Arc is responsible for dynamin activation.

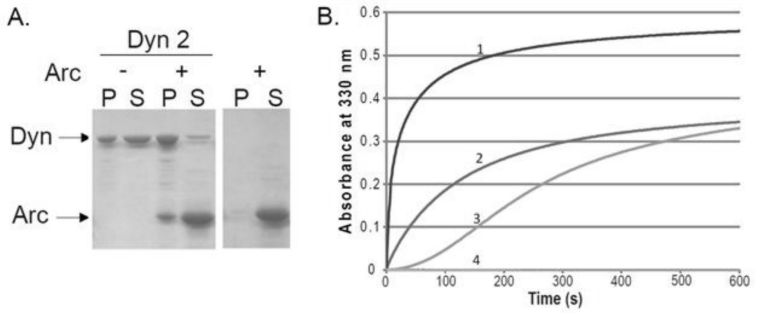

Figure 1. Interaction of Arc with Dyn2 as measured by co-sedimentation and turbidity

A. Binding of Arc to Dyn2 polymers. Polymerization of Dyn2 (final concentration of 1 μM) was induced by lowering the NaCl concentration from 300 mM to 75 mM, and incubating for 15 min at 22°C in the absence or presence of Arc (4 μM). Samples were then centrifuged at 214,000 × *g* for 15 min at 4°C. Pellets were resuspended in the initial sample volume and equal volumes of pellets (P) and supernatants (S) were subjected to SDS-PAGE and Coomassie blue staining. The right panel shows the results with 4 μM Arc alone. B. Time course of polymerization, measured by the absorbance at 330 nm, of Dyn2 (final concentration of 0.6 μM) upon dilution from 300 mM NaCl to 75 mM NaCl, in the absence of Arc (curve 3) and in the presence of 0.1 μM Arc (curve 2) or 1 μM Arc (curve 1). Curve 4 shows 1 μM Arc alone.

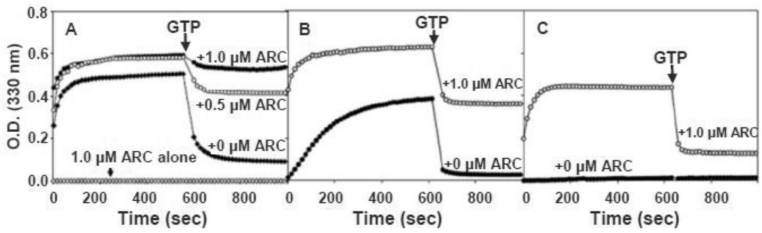

Figure 2. Enhancement of Dyn2 assembly by Arc

A. Absorbance traces showing Dyn2 polymerization upon reduction of NaCl concentration from 300 mM to 50 mM in the absence of Arc or in the presence of 0.5 μM or 1 μM Arc, as designated in the figure. B. Dyn2 polymerization in the presence of 1 μM Arc in buffer containing 75 mM NaCl. C. Dyn2 polymerization in the presence of 1 μM Arc in buffer containing 100 mM NaCl. Arrows designate addition of $MgCl_2$ and GTP to final concentrations of 2 mM and 1 mM, respectively. In all cases, the Dyn2 concentration was 1 μM, the temperature was 37°C, and the absorbance was measured at 330 nm.

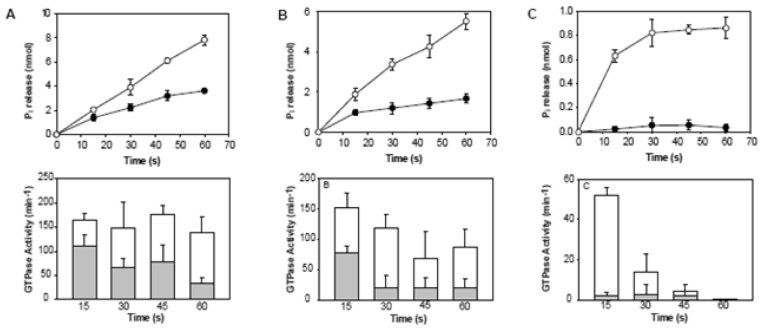

Figure 3. Stimulation of the GTPase activity of Dyn2 by Arc

Top panels show the time courses of GTP hydrolysis catalyzed by 1 μM Dyn2 in the absence (●) or presence (○) of 1 μM Arc, measured at 37°C in buffer containing 50 mM NaCl (A), 75 mM NaCl (B), or 100 mM NaCl (C). Bottom panels show the decrease in specific activities at each NaCl concentration over 1 min time courses in the absence (shaded bars) or presence (open bars) of Arc. Each bar represents the activity measured over the 15 seconds prior to the times designated on the abscissa. Less than 10% of substrate (GTP) was depleted in all measurements. Data represent the mean +/− SD of triplicate measurements from two experiments.

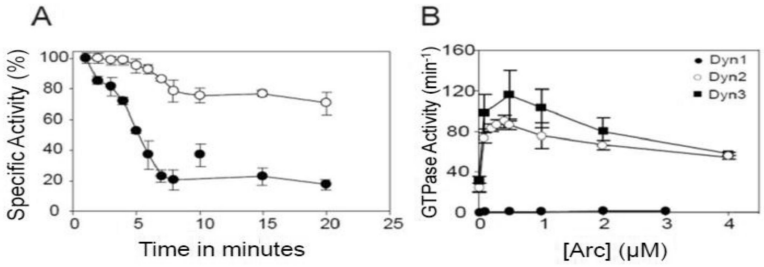

Figure 4. Stabilization of the high-activity state of Dyn2 by Arc

A. GTPase activity of Dyn2 (0.1 μM) was measured for various times in 50 mM NaCl at 37°C in the absence (●) or presence (○) of 0.5 μM Arc. Each value corresponds to the percent of maximal specific activity measured over the interval between time points. Under these assay conditions, the activities of Dyn2 in the absence and presence of Arc were ~25 min^{-1} and ~90 min^{-1}, respectively. Data represent the mean +/− SD of triplicate measurements. B. GTPase activities of Dyn1 (●), Dyn2 (○), and Dyn3 (■) at concentrations of 0.1 μM, were measured for 20 min in 50 mM NaCl at 37°C as a function of Arc concentration.

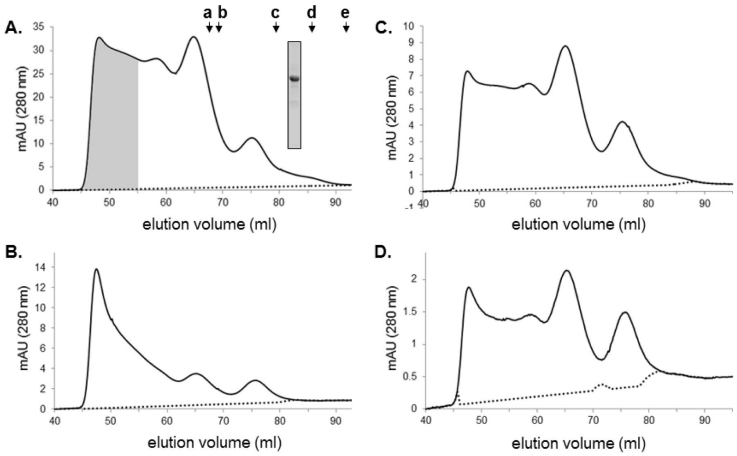

Figure 5. Size-exclusion chromatography of Arc on a Superdex 200 column

A. Elution profile of untagged Arc (0.5 ml of 45 μM Arc in buffer B). Inset shows the Coomassie blue-stained gel of the loaded sample. Arrows above the profile designate standards: a. β-amylase (Stokes' radius 5.4 nm), b. catalase (5.2 nm), c. BSA (3.6 nm), d. ovalbumin (3.1 nm), e. carbonic anhydrase (2.4 nm). Void volume and total volume of the column are 40 ml and 110 ml, respectively. B. Elution profile of fractions 44-54 from panel A (shaded), concentrated and then re-chromatographed on the same column. C and D. Elution profiles of 1 μM and 0.25 μM Arc, respectively (4-fold and 16-fold dilutions of the sample chromatographed in panel A).

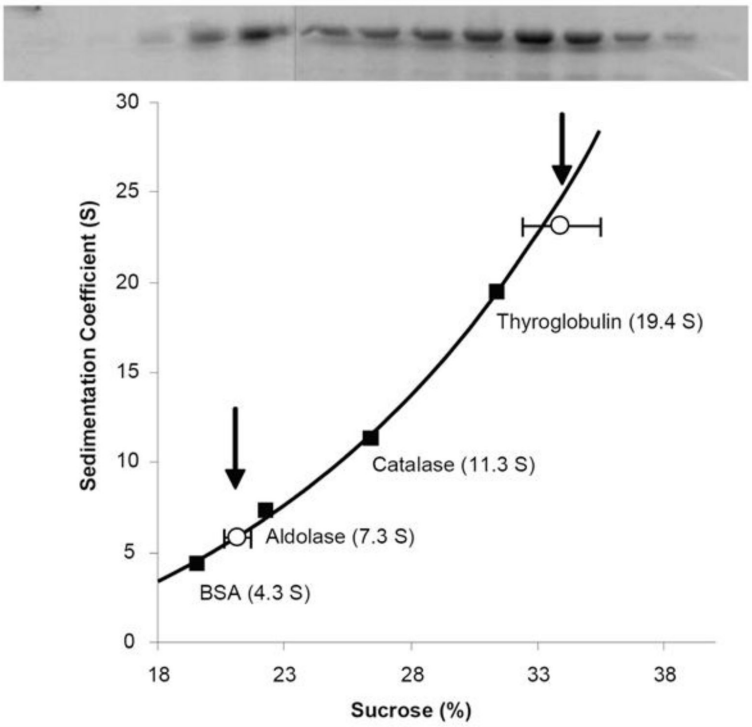

Figure 6. Sucrose density gradient centrifugation of Arc

His_6-Arc (20 μM, 0.4 ml) was layered above a 4 ml 10-40% sucrose gradient and centrifuged at 240,000 × *g* for 16 h at 4°C. Following centrifugation, fractions were subjected to SDS-PAGE and Coomassie blue staining (top panel). Standard proteins were centrifuged under identical conditions to generate a plot of sedimentation coefficient (S) as a function of sucrose concentration, as measured by refractometry (bottom panel). The data shown are representative of 4 measurements performed using two Arc preparations.

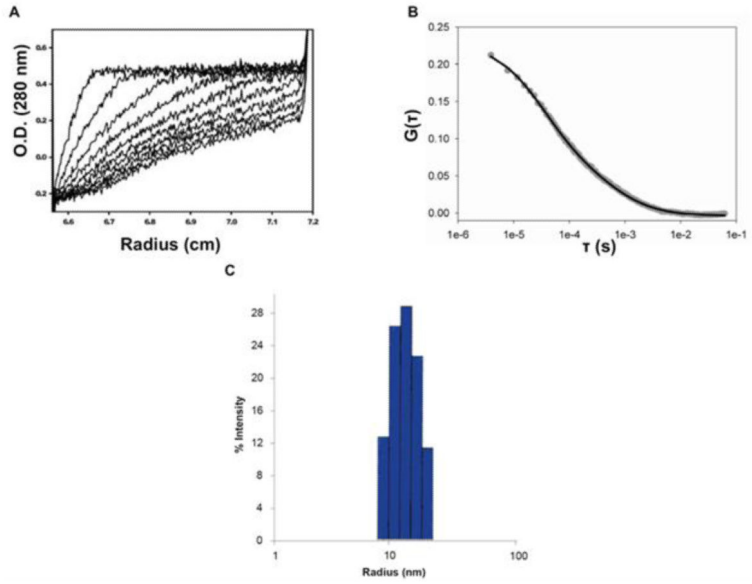

Figure 7. Hydrodynamic analysis of Arc

A. Sedimentation velocity analysis. Experiments were carried out in a Beckman XL-I analytical ultracentrifuge at 20°C, and 35,000 rpm and an Arc concentration of 36 μM. The figure shows UV scans (at 280 nm), taken every four min, from a representative run. B. Fluorescence correlation spectroscopy. Autocorrelation curve of 150 nM Arc-AF488 (grey circles) and fit to data (black line). The results of the fit were D_1 = 22 $\mu m^2/s$ (G_0 = 0.066), D_2 = 430 $\mu m^2/s$ (G_0 = 0.15). C. Dynamic Light Scattering. A solution of Arc (16 μM) was introduced into a Wyatt DynoPro DLS instrument and attached temperature Controlled MicroSampler pre-equilibrated to 4°C. The data shown are representative of six measurements, each consisting of thirty 10 second scans at 90% laser intensity. The resulting peak accounts for >99.7% of the mass and >90% of the intensity.

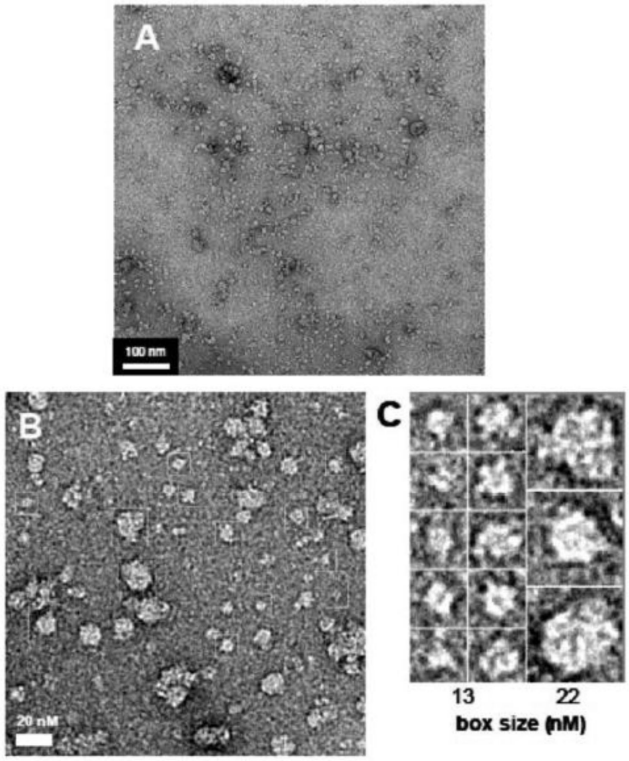

Figure 8. Imaging of Arc by transmission electron microscopy

His_6-Arc was negatively stained and imaged at 50,000 x magnification as described in Materials and Methods. Bars (in panels A and B) and box sizes (in panel C) designate dimensions in nm.

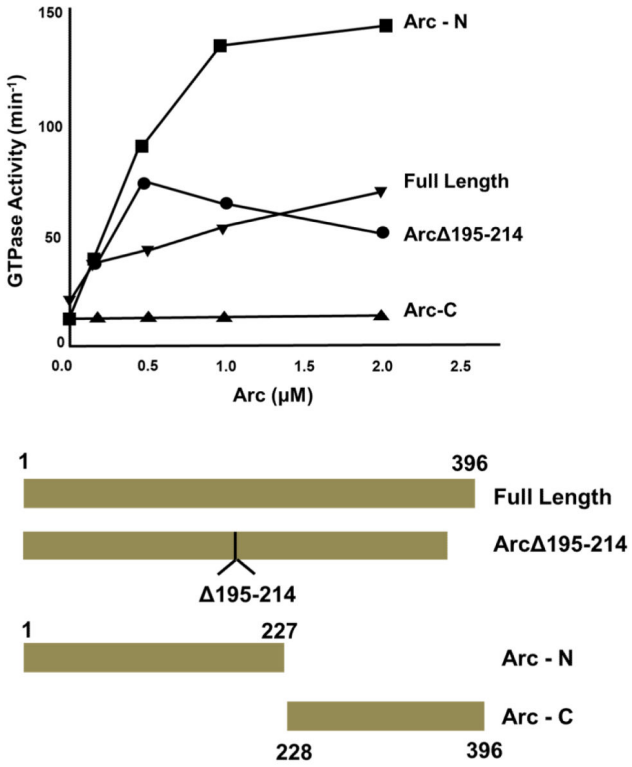

Figure 9. Identification of Dyn2 activation determinants in Arc

GTPase assays, performed as described in Figure 4, were carried out in the presence of full-length Arc (residues 1-396), a fragment lacking the putative Dyn2 binding site (Arc-Δ195-214), an N-terminal fragment comprising residues 1- 227 (Arc-N), and a C-terminal fragment comprising residues 228-396 (Arc-C). A scheme of the fragments tested is shown below.